

Homeotropic and Planar Alignment of Discotic Liquid Crystals: The Role of the Columnar Mesophase

Guillaume Schweicher, Gabin Gbabode, Florence Quist, Olivier Debever,
Nicolas Dumont, Sergey Sergeev, and Yves H. Geerts*

Laboratoire de Chimie des Polymères, Faculté des Sciences, Université Libre de Bruxelles (ULB),
CP206/1, Boulevard du Triomphe, 1050 Brussels, Belgium

Received August 26, 2009. Revised Manuscript Received October 26, 2009

Blends of two metal-free phthalocyanine mesogens exhibiting different mesophases (Col_r phase from room temperature to isotropization for the first one, and Col_r at room temperature then Col_h from around 60 °C to isotropization for the second one) have been studied in order to determine the relationship between the type of mesophase and the alignment behavior. The phase diagram of this system has been built and evidence of full solid-state miscibility of the two pure constituents in all proportions and temperatures is presented. Investigation of phase alternation at room temperature as a function of composition revealed that border compositions exhibit Col_r phases similar to the pure constituents, whereas Col_h mesophase was stabilized for intermediate compositions. Combined polarized optical microscopy observations and X-ray diffraction measurements showed that homeotropic alignment is adopted only for mixed samples exhibiting Col_h mesophase, thus demonstrating that the presence of a Col_h mesophase is a necessary condition for homeotropic alignment.

Introduction

Organic semiconductors have aroused much interest in the past few years¹ and among the different materials under study, π -conjugated liquid crystals have attracted particular attention due notably to their self-assembling ability, their malleability and their ease of processing. Generally speaking, there exist two types of liquid crystalline mesogens, which differ not only in their shape, but also in the type of self-assembled structure they yield and in the dimensionality of charge transport and exciton migration within such structures.¹ Rod-shaped calamitics can form nematic (orientational order) or smectic (orientational as well as positional order) phases and present a two-dimensional charge transport in directions perpendicular to the long axis of the molecules. In addition to forming nematic mesophases, disk-shaped discotics can self-assemble into columns, which can then arrange into a hexagonal, a rectangular, a tetragonal, an oblique, or a cubic lattice.² Charge transport in such columnar mesophases is one-dimensional and its direction is parallel to the column axis. To construct efficient devices, it is therefore necessary to control the self-assembled structures formed by such materials and, in particular, to control the charge transport direction relating to the alignment of the mesophase. Although the alignment of low-molecular-weight calamitic nematic

mesophases onto surfaces, through rubbing or photo-alignment techniques in particular, has been extensively studied (notably because of their use in liquid crystal displays, LCD^{2-4}), the alignment of discotic columnar mesophases has not received as much attention. The latter can present two types of alignment with respect to a substrate: planar alignment, in which the column axes lie parallel to the surface and homeotropic alignment where the column axes are perpendicular to the surface. These two orientations can be used in different applications. For example, uniaxial planar orientation is needed for field-effect transistors applications, whereas homeotropic alignment can be used in solar cells or light-emitting diodes.¹

A few examples of induced alignment of discotic columnar mesophases, through construction of Langmuir–Blodgett thin films,^{5,6} zone-casting techniques,^{7–9} photopatterning¹⁰ or use of magnetic fields¹¹ have been reported

*Corresponding author. E-mail: ygeerts@ulb.ac.be.

(1) Sergeev, S.; Pisula, W.; Geerts, Y. H. *Chem. Soc. Rev.* **2007**, *36*, 1902–1929.
(2) Laschat, S.; Baro, A.; Steinke, N.; Giesselmann, F.; Hägele, C.; Giusy Scalia, G.; Judele, R.; Kapatsina, E.; Sauer, S.; Schreivogel, A.; Tosoni, M. *Angew. Chem., Int. Ed.* **2007**, *46*, 4832–4887.

(3) Hoogboom, J.; Elemans, J. A. A. W.; Rasing, T.; Rowan, A. E.; Nolte, R. J. M. *Polym. Int.* **2007**, *56*, 1186–1191.
(4) Ichimura, K. *Chem. Rev.* **2000**, *100*, 1847–1873.
(5) Bonosi, F.; Ricciardi, G.; Leij, F.; Martini, G. *J. Phys. Chem.* **1993**, *97*, 9181–9186.
(6) Maliszewskij, N. C.; Heiney, P. A.; Josefowicz, J. Y.; Plesniviy, T.; Ringsdorf, H.; Schuhmacher, P. *Langmuir* **1995**, *11*, 1666–1674.
(7) Pisula, W.; Tomović, Ž.; Stepputat, M.; Kolb, U.; Pakula, T.; Müllen, K. *Chem. Mater.* **2005**, *17*, 2641–2647.
(8) Tracz, A.; Makowski, T.; Masirek, S.; Pisula, W.; Geerts, Y. H. *Nanotechnology* **2007**, *18*, 485303–485307.
(9) Miszkiewicz, P.; Rybak, A.; Jung, J.; Glowacki, I.; Ulanski, J.; Geerts, Y. H.; Watson, M.; Mullen, K. *Synth. Met.* **2003**, *137*, 905–906.
(10) Furumi, S.; Janietz, D.; Kidowaki, M.; Nakagawa, M.; Morino, S.; Stumpe, J.; Ichimura, K. *Chem. Mater.* **2001**, *13*, 1434–1437.
(11) Eichhorn, S. H.; Adavelli, A.; Li, H. S.; Fox, N. *Mol. Cryst. Liq. Cryst.* **2003**, *397*, 347–358.

in the literature; however, spontaneous alignment, obtained without application of external forces, is still poorly understood. From previous studies led by Grelet and Bock,¹² spontaneous alignment of discotic columnar phases seems to depend strongly on the air–liquid crystal (LC) interface. This is supported by the fact that some mesogens can form one type of alignment when sandwiched between two substrates and another one on a single substrate.¹³ However, it has been proven for phthalocyanine discotic liquid crystals that the chemical composition and surface tension of solid substrates with low roughness play no role on alignment, as homeotropic alignment has been observed for hydrophilic, lyophobic, fluorophilic and metallic surfaces.¹³ Other factors such as molecular structure, annealing temperature, cooling rate and purity have also been investigated in order to get further understanding of the alignment phenomenon but no particular trends could be discerned.^{1,3,12,14–20} Although several factors contribute to the alignment process, a survey of the literature shows that all reported homeotropic alignments seem to coincide with the existence of a columnar hexagonal (Col_h) phase.^{7,12,13,15,21–28} However, the following question has never been, to the best of our knowledge, explicitly addressed in the available literature reports: does the type of mesophase influence the alignment behavior? This article intends to evidence a clear relationship between mesophase type and alignment behavior. Toward this end the spontaneous alignment of thick films on one substrate and between two substrates was systematically studied for blends of two miscible phthalocyanine mesogens possessing different thermotropic behavior.

Experimental Section

The synthesis of compounds **1** and **2** is described in previous publications by our group.^{29–31} Blends of **1** and **2** were made by weighing appropriate amounts of the two compounds, solubilizing in dichloromethane and then evaporating the solvent under reduced pressure. Fifteen blends of different compositions (defined as the molar fraction (x) of compound **2** in a blend) varying from 0 to 1 were prepared.

Thermal transitions were determined by differential scanning calorimetry (DSC) performed using a Pyris DSC Diamond (Perkin-Elmer) at a scanning rate of 20 °C/min. Three heating/cooling cycles were performed on two different samples for each composition. First scans were discarded because of the fact that these are dependent on the thermal history of the sample. Average of the onset temperatures was determined for the transitions of the consecutive scans. Onset temperatures could not be determined manually for compositions $x = 0.05–0.15$ because of the extreme broadness of the isotropization peak. Estimation of the transition temperature was then performed. See the Supporting Information for related calculation of these transition temperatures.

Optical textures were observed with a polarizing microscope (Nikon Eclipse 80i) equipped with a hot stage (Linkam Scientific Instruments, CI94). All samples were prepared on precleaned glass slides. Powder X-ray diffraction measurements were performed on a Bruker D8 Advance diffractometer using Cu K α radiation ($\lambda = 1.5418 \text{ \AA}$). All samples were prepared on thin precleaned aluminum plates (rugosity rms: 0.3 μm , contact angle with water: 92°). The material was spread on the aluminum substrate to form a uniform layer (thickness of a few hundreds of micrometers) to avoid additional broadening of diffraction peaks. Diffraction patterns were collected in the scattered angular range between 1.6° and 30° with an angular resolution of 0.02° per step and a typical counting time of 10 s per step, using Bragg–Brentano geometry (θ/θ setup). X-ray diffraction patterns are represented as the scattering intensity versus 2θ (in degrees), the angle between incident and diffracted X-ray beams. Sample temperature was controlled within 0.1 °C accuracy.

Results

1. Thermotropic Behavior of Pure Constituents. Prior to constructing the phase diagram of the blends, we analyzed the two pure constituents **1** and **2** (Scheme 1). The phase transitions observed by DSC and XRD for both compounds corresponded to those reported previously.^{29–31} Compound **1** showed Col_r–isotropization at 151.6 °C (8.18 kJ mol⁻¹), whereas compound **2** exhibited a Col_r–Col_h transition at 58.3 °C (0.07 kJ mol⁻¹) and Col_h–isotropization at 181.6 °C (4.8 kJ mol⁻¹). For compound **2**, higher transition temperatures than those found in the literature^{22,29,31,32} are observed because of a higher purity of samples used in this study. Plane group $c2mm$ (Figure 1, left) had been ascribed to both Col_r phases **1** and **2** in previous publications.^{29–31}

- (12) Grelet, E.; Bock, H. *Europhys. Lett.* **2006**, *73*, 712–718.
 (13) De Cupere, V.; Tant, J.; Viville, P.; Lazzaroni, R.; Osikowicz, W.; Salanek, W. R.; Geerts, Y. H. *Langmuir* **2006**, *22*, 7798–7806.
 (14) Kaslter, M.; Pisula, W.; Laquai, F.; Kumar, A.; Davies, R. J.; Balushev, S.; García-Gutiérrez, M.-C.; Wasserfallen, D.; Butt, H.-J.; Riekel, C.; Wegner, G.; Müllen, K. *Adv. Mater.* **2006**, *18*, 2255–2259.
 (15) Pisula, W.; Tomovic, Z.; El Hamaoui, B.; Watson, M. D.; Pakula, T.; Müllen, K. *Adv. Funct. Mater.* **2005**, *15*, 893–904.
 (16) Kumar, S. *Chem. Soc. Rev.* **2006**, *35*, 83–109.
 (17) Hatsusaka, K.; Ohta, K.; Yamamoto, I.; Shirai, H. *J. Mater. Chem.* **2001**, *11*, 423–433.
 (18) Hoogboom, J.; Garcia, P. M. L.; Otten, M. B. J.; Elemans, J. A. A. W.; Sly, J.; Lazarenko, S. V.; Rasing, T.; Rowan, A. E.; Nolte, R. J. M. *J. Am. Chem. Soc.* **2005**, *127*, 11047–11052.
 (19) Yoshio, M.; Kagata, T.; Hoshino, K.; Mukai, T.; Ohno, H.; Kato, T. *J. Am. Chem. Soc.* **2006**, *128*, 5570–5577.
 (20) Sergeev, S.; Levin, J.; Balandier, J.-Y.; Pouzet, E.; Geerts, Y. H. *Mendeleev Commun.* **2009**, *19*, 185–186.
 (21) Charlet, E.; Grelet, E.; Brettes, P.; Bock, H.; Saadaoui, H.; Cisse, L.; Destruel, P.; Gherardi, N.; Seguy, I. *Appl. Phys. Lett.* **2008**, *92*, 024107.
 (22) Gearba, R. I.; Anokhin, D. V.; Bondar, A. I.; Bras, W.; Jahr, M.; Lehmann, M.; Ivanov, D. A. *Adv. Mater.* **2007**, *19*, 815–820.
 (23) Terasawa, N.; Monobe, H.; Kiyohara, K.; Shimizu, Y. *Chem. Commun.* **2003**, 1678–1679.
 (24) Terasawa, N.; Tanigaki, N.; Monobe, H.; Kiyohara, K. *J. Fluorine Chem.* **2006**, *127*, 1096–1104.
 (25) Pisula, W.; Kaslter, M.; El Hamaoui, B.; García-Gutiérrez, M.-C.; Davies, R. J.; Riekel, C.; Müllen, K. *Phys. Chem. Phys.* **2007**, *8*, 1025–1028.
 (26) Kang, S.-W.; Lui, Q.; Chapman, B. D.; Pindak, R.; Cross, J. O.; Li, L.; Nakata, M.; Kumar, S. *Chem. Mater.* **2007**, *19*, 5657–5663.
 (27) Kroon, J. M.; Koehorst, R. B. M.; van Dijk, M.; Sanders, G. M.; Sudhölter, J. R. J. *Mater. Chem.* **1997**, *7*, 615–624.
 (28) Ichihara, M.; Miida, M.; Mohr, B.; Ohta, K. *J. Porphyrins Phthalocyanines* **2006**, *10*, 1145–1155.

- (29) Tant, J.; et al. *J. Phys. Chem. B* **2005**, *109*, 20315–20323.
 (30) Sergeev, S.; Pouzet, E.; Debever, O.; Levin, J.; Gierschner, J.; Cornil, J.; Aspe, R. G.; Geerts, Y. H. *J. Mater. Chem.* **2007**, *17*, 1777–1784.
 (31) Tant, J.; et al. *J. Phys. Chem. B* **2006**, *110*, 3449.
 (32) Gearba, R. I.; Bondar, A. I.; Goderis, B.; Bras, W.; Ivanov, D. A. *Chem. Mater.* **2005**, *17*, 2825–2832.

Scheme 1. Molecular Structure and Properties of Mesogenic Phthalocyanines

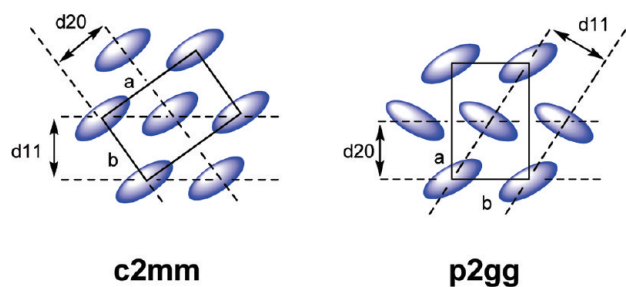
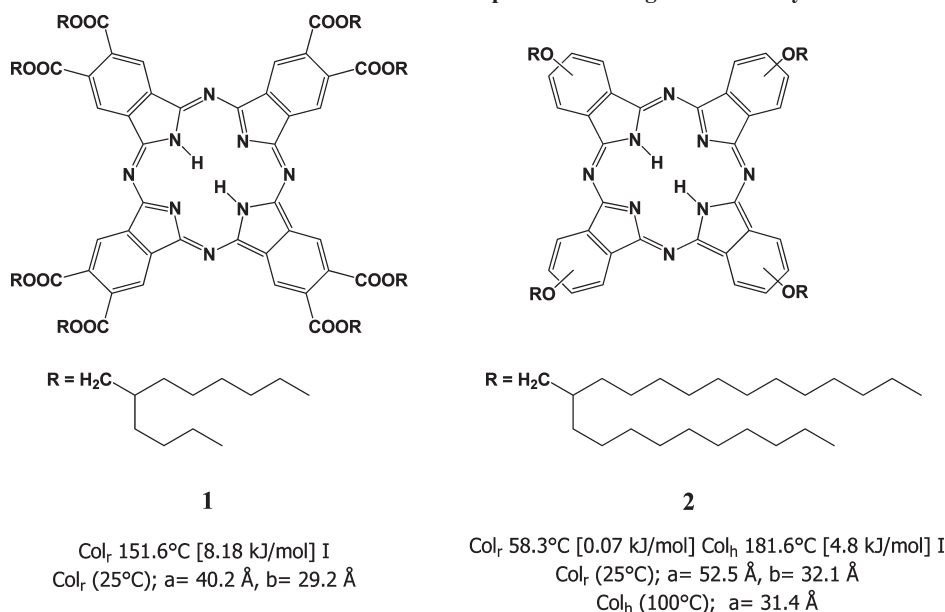


Figure 1. Schematic representation of Col_r unit cells of **1** and **2** (c2 mm). Unit cell with p2gg symmetry is shown for comparison.

2. Thermotropic Behavior of Blends. Compiling the transition temperatures obtained by DSC analysis as a function of composition allowed us to obtain a phase diagram of the binary system (Figure 2). The smooth, continuous evolution of transition temperature with composition is a clear indication of the full solid-state miscibility of both compounds and this conclusion is reinforced by the observation that transition temperatures upon heating and cooling are superimposed (see Figure S1 in the Supporting Information). Such solid-state miscibility was expected because of the fact that the two phthalocyanine mesogens used in this study present similar backbones, and has already been observed in the case of other mesogens blends.^{33–35} Conspicuous also is the rapid disappearance of the Col_r–Col_h transition, which was only observed for molar fractions of **2** above 0.925, that is, minimal addition of compound **1** to compound **2**. This transition occurs over a large temperature

range for mole fractions 0.925 and 0.95 and could be observed only by POM and XRD (Figure 2 and S2). All other compositions presented only one transition corresponding to isotropization.

Three main regions can be discerned in this phase diagram: compositions from $x = 0.975$ to $x = 0.925$, from $x = 0.90$ to $x = 0.40$ and from $x = 0.30$ to $x = 0.05$.

X-ray powder diffraction patterns have been measured at room temperature for each composition in order to investigate the evolution of the structural arrangement as a function of composition. Figure 3 shows the evolution of the low-angle region of the X-ray diffraction patterns measured at room temperature as a function of composition from **1** to **2**. The three above-mentioned domains of composition can also be recognized here through different trends in the evolution of the position and intensity of the diffraction peaks. The cell parameters determined for all compositions, together with observed and calculated positions of hk reflections, can be found in the Supporting Information.

Compositions from $x = 0.975$ to $x = 0.925$. X-ray diffraction patterns measured for these compositions are very similar to the one of the Col_r phase of **2**. Two intense partially overlapping diffraction peaks are visible in the 3–4° 2θ range which have been indexed as 11 and 20 reflections, as for **2**. Higher order reflections are also present between 5° and 7° with similar positions and relative intensities to **2** and can be given the same hk indices (see Table S2 and Figure S3 in the Supporting Information). This indicates that compositions from $x = 0.975$ to $x = 0.925$ exhibit a Col_r phase similar to that of **2** at room temperature. However, a gradual translation of the 20 reflection toward lower angles is observed from $x = 0.975$ to 0.925, which implies a continuous increase in the a parameter (see Table S2 in the Supporting Information). Plane group $c2mm$ can be attributed to the Col_r phase of these blends as in the case of compound **2**.

(33) Zucchi, G.; Donnio, B.; Geerts, Y. H. *Chem. Mater.* **2005**, *17*, 4273–4277.

(34) Zucchi, G.; Viville, P.; Donnio, B.; Vlad, A.; Melinte, S.; Mondeshki, M.; Graf, R.; Spiess, H. W.; Geerts, Y. H.; Lazzaroni, R. *J. Phys. Chem. B* **2009**, *113*, 5448–5457.

(35) Neubert, M. E. In *Liquid Crystals, Experimental Study of Physical Properties and Phase Transitions*; Kumar, S., Ed.; Cambridge University Press: Cambridge, U.K., 2001; p 32.

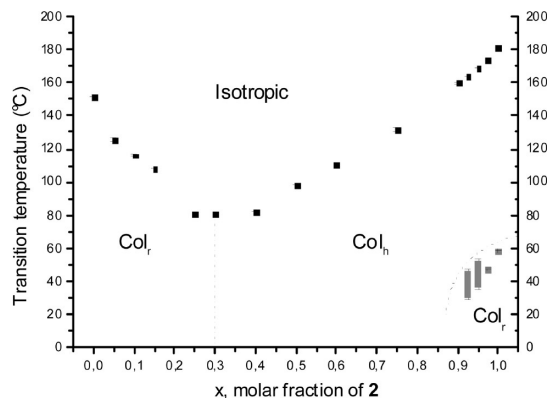


Figure 2. Phase diagram of binary system **1** and **2**. Gray strips represent Col_r - Col_h transition temperature range.

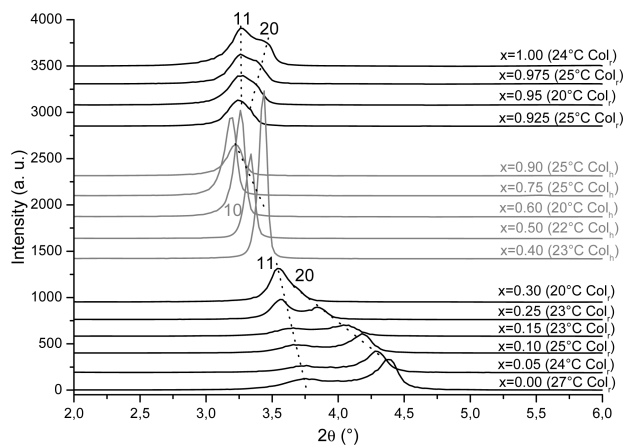


Figure 3. Evolution, as a function of composition, of the low-angle region ($2-6^\circ 2\theta$ range) of the X-ray diffraction patterns measured at room temperature.

X-ray powder diffraction measurements as a function of temperature confirmed that these three compositions all undergo Col_r to Col_h transition when temperature increases. The X-ray diffraction patterns measured at 70°C for these three compositions all show a sharp intense peak at low scattering angle followed by three additional higher-order less intense peaks. Reticular distances of the observed reflections follow a ratio $1:1/\sqrt{3}:1/2:1/\sqrt{7}$, which is typical of the Col_h phase of **2**.^{29,31} It is therefore apparent that the structural behavior of compositions 0.975–0.925 is similar to that of compound **2**.

Compositions from $x = 0.90$ to $x = 0.40$. When the amount of **1** is further increased, Col_h arrangement is stabilized at room temperature. X-ray diffraction patterns of compositions $x = 0.90$ and $x = 0.75$ measured at room temperature exhibit the same characteristic peaks observed for the high temperature Col_h phase of compositions from $x = 1.00$ to $x = 0.925$ (see Figure S4 and Table S3 in the Supporting Information). For compositions from $x = 0.60$ to $x = 0.40$, the higher order diffraction peaks are no longer visible, but a sharp strong intense peak (10 reflection) is still present at low angles, indicating a Col_h arrangement. We hypothesize that a random distribution of molecules of **1** within the columns is detrimental to the occurrence of higher order

diffraction peaks. Compositions from $x = 0.90$ to $x = 0.40$ all exhibit a Col_h phase at room temperature. Only one transition from Col_h to isotropic is observed by DSC (see Table S1 in the Supporting Information).

Compositions from $x = 0.30$ to $x = 0.05$. For composition $x = 0.30$, the 10 reflection, observed until $x = 0.40$, is now split into two convoluted reflections. From $x = 0.30$ to $x = 0.05$ the positions and relative intensities of these two diffraction peaks evolve so that they nearly match those observed for **1** at $x = 0.05$. These two reflections have been attributed to the same hk indices as for **1** (see Table S4 in the Supporting Information). Furthermore, the 13 reflection, which is observed for **1**, is also present for compositions from $x = 0.15$ to $x = 0.05$. This clearly indicates that they exhibit a similar Col_r phase and also allows us to conclude that these phases have $c2mm$ symmetry. The 13 reflection is no longer observed for compositions $x = 0.30$ to $x = 0.25$, probably because of random distribution of compound **2** within the columns.

*Solid-State Miscibility of Compounds **1** and **2**.* When looking at X-ray diffraction patterns of all compositions at room temperature, coexistence of diffraction peaks belonging to two different columnar arrangements is never observed. This constitutes clear evidence that no phase separation occurs in the entire composition range and that the two compounds are miscible in all proportions at the solid state. This is in agreement with the absence of invariant transition in DSC. Instead, a continuous transition, from Col_r to Col_h and from Col_h to Col_r , is observed on increasing x . It is further demonstrated by the continuous evolution of the position and intensities of the diffraction peaks for blends from **1** to **2** and supported by the evolution of the surface per molecule ratio (S/Z) calculated from the cell parameters ($S = ab$ and $Z = 2$ for the Col_r phases, $S = a^2(\sqrt{3}/2)$ and $Z = 1$ for the Col_h phases), which is shown in Figure S5 of the Supporting Information. To summarize and rationalize the phase alternation at room temperature in this binary mixture, we give the evolution of cell parameters as a function of composition in Figure 4 (a_r and b_r refer to cell parameters of Col_r phases, and a_h to cell parameter of Col_h phases). The three above-mentioned zones are again well distinguished in this representation. In the two Col_r domains, a similar trend is observable: b_r remains constant, whereas a_r increases continuously upon addition of the other constituent. For the Col_h domain, which lies between the two above-mentioned Col_r domains, a small continuous increase of a_h with x from the b_r value of $x = 0.30$ (limit of the Col_r domain of **1**) to the b_r value of $x = 0.925$ (limit of the Col_r domain of **2**) is noticeable. Transitions from Col_r to Col_h as a function of composition can then be rationalized by a continuous distortion of the rectangular lattice. Indeed, the cell parameter b_r is almost equal to a_h , and a_r increases until reaching the value of $a_h\sqrt{3}$. This value corresponds to the length of the rectangular cell that can be built in a hexagonal lattice (Figure 4). For the two boundary compositions (Col_r - Col_h border) $x = 0.30$ and $x = 0.925$, the a_r/b_r ratio is indeed almost equal to $\sqrt{3}$ (relative error less than

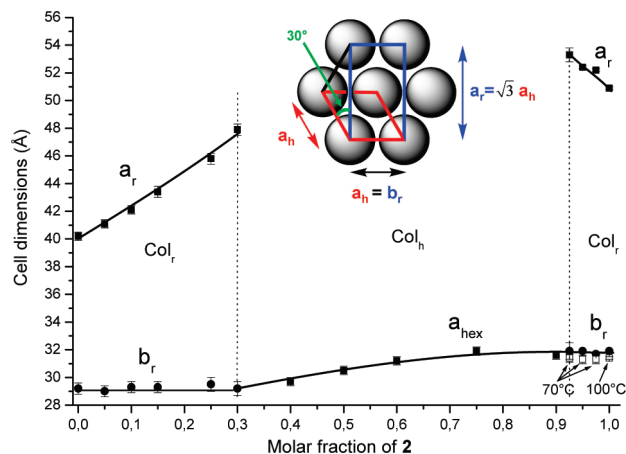


Figure 4. Evolution of the cell parameters determined at room temperature, as a function of composition. a_r and b_r refer to cell parameters of Col_r phases, and a_h to cell parameter of Col_h phase. White squares correspond to cell parameters of high temperature Col_h phase. The figure in the middle is a schematic representation of a hexagonal arrangement of discotic molecules (the axis of the columns is perpendicular to the plane of the figure). The hexagonal unit cell is drawn in red and the rectangular unit cell, which can also be built from this arrangement, is in blue.

5%). This composition-dependent Col_r – Col_h transition is similar to the temperature-dependent Col_r – Col_h transition observed for **2** and for the blends with compositions from $x = 0.925$ to $x = 0.975$ (see Figure S1 in the Supporting Information). For the latter compounds in particular, the values of a_h of the high-temperature Col_h phase (open squares in Figure 4) are very close to those of b_r of the room-temperature Col_r phase.

The shape of the experimental phase diagram found, i.e., the isotropization curve going through a minimum, is expected for a blend of two compounds with similar crystal structures and a dimensional factor³⁶ higher than 15% (Hume–Rothery rule³⁷). It is assumed that such difference in the size of the components introduces into the solid solution a lattice strain energy which is not present in the liquid solution, thus giving a tendency to stabilize the liquid rather than the solid state.⁵ In the present case, **1** and **2** do present a dimensional factor higher than 15% (estimated using Chem3D). The minimum is situated close to $x = 0.30$, which indicates that the aforementioned lattice strain energy is the highest at the Col_r – Col_h transition in molar fractions.

3. Alignment between Two Substrates. Textures of the binary mixtures confined between two glass substrates were observed by POM (Figure 5). Samples are several centimeters wide and a few micrometers thick. Therefore, no edge effects have been observed. As has been stated previously, compound **2** tends to align homeotropically when confined between two substrates, whereas compound **1** adopts planar alignment. This is visible through the absence of texture for annealed compound **2** and by the typical fan-like texture for annealed compound **1**.

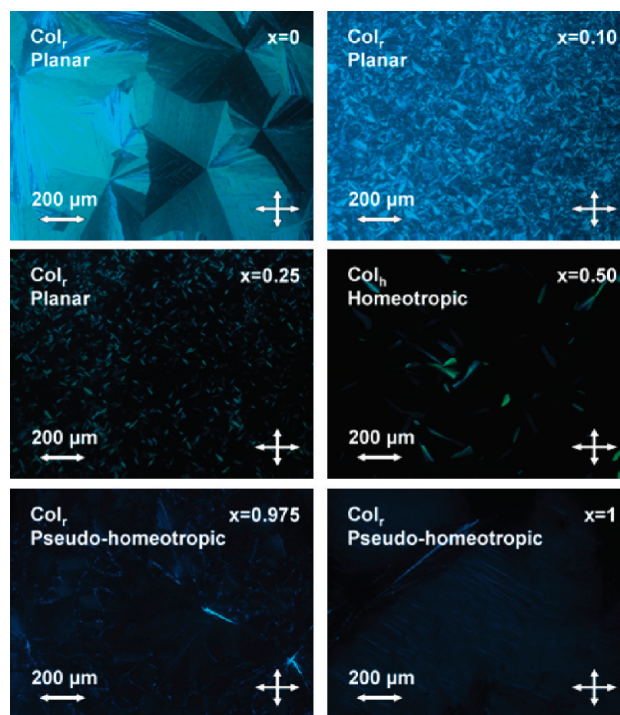


Figure 5. POM textures of different blends between two substrates. Images taken at room temperature.

In agreement with the phase diagram, it is possible to discern three different behaviors.

Above $x = 0.925$, a pseudohomeotropic^{13,38} alignment as in pure **2** is observed.

From $x = 0.90$ to $x = 0.40$, where the Col_h –isotropization transition occurs, homeotropic alignment is observed. This alignment is characterized by an absence of texture (image appears black because the optical axis is equivalent to the columnar axis and to the normal of the disklike molecules, which cancels out any birefringence phenomena). Only a few defects, probably due to dust particles present on the original glass slides, are observed.

Finally, for concentrations between $x = 0.30$ and $x = 0.05$, where only a Col_r –isotropization transition occurs, fanlike texture typical of planar arrangement is observed. It is, however, apparent that domain sizes become smaller as the concentration increases. In this concentration range, compound **2** acts as an impurity that destabilizes the Col_r mesophase of compound **1**. At concentrations of 0.30 and 0.25, the typical fanlike texture is no longer obvious, but can still be observed at higher magnification in the remaining birefringent areas.

4. Alignment on One Substrate. POM images taken on one single substrate showed planar alignment upon annealing for both pure compounds, **1** and **2** (Figure 6). This has also been established by X-ray diffraction by comparison of patterns measured at room temperature before and after isotropization. By analyzing the evolution of the relative intensities of the characteristic peaks (2 – 5°

(36) The dimensional factor is defined as the ratio of the molecular diameter D of the constituents. So, in our case dimensional factor is $(D_2 - D_1)/D_2$.

(37) Prince, A. In *Alloy Phase Equilibria*; Elsevier: Amsterdam, 1966; Chapter III.

(38) Pouzet, E.; De Cupere, V.; Heintz, C.; Andreasen, J. W.; Breiby, D. W.; Nielsen, M. M.; Viville, P.; Lazzaroni, R.; Gbabode, G.; Geerts, Y. H. *J. Phys. Chem. C* **2009**, *113*, 14398–14406.

2θ angle region) between the two experiments, one can qualitatively assess the molecular alignment.^{8,39}

Figure 7 shows a superposition of the low-angle region of X-ray diffraction patterns measured at room temperature before and after isotropization for **1** (Figure 7a) and **2** (Figure 7b). For both compounds, significant changes of the relative intensities of the 11 and 20 reflections are observed, which is different for the two compounds. In the case of compound **1** the intensity of the 11 reflection overwhelms that of the 20 reflection after isotropization. The opposite can be seen for compound **2**. Moreover, only the second order of the most intensive reflections is observed at higher angles in each case (not shown). This

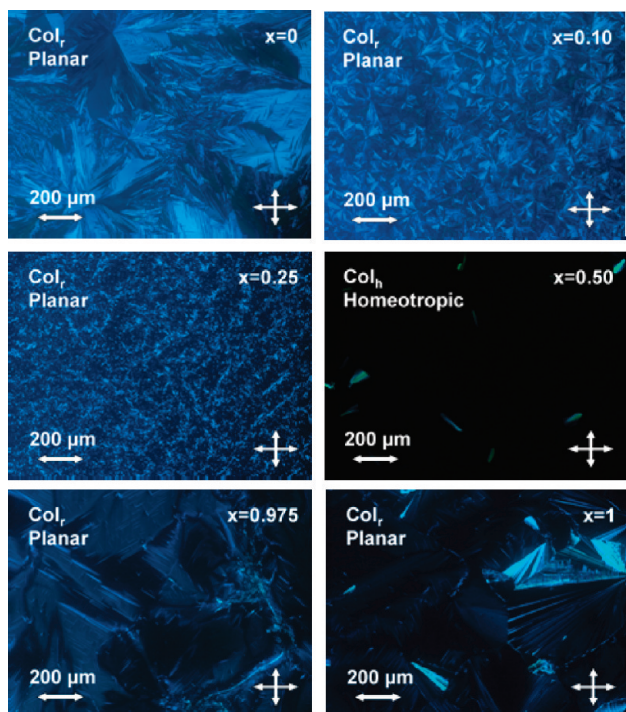


Figure 6. POM textures of different blends on one substrate. Images taken at room temperature.

implies that both compounds exhibit a planar alignment with a well-defined orientation of the 2D rectangular unit cell toward the substrate: along its diagonal for **1**, 11 planes being parallel to the substrate and along its short side for **2**, 20 planes being parallel to the substrate (insets in Figure 7). Note that these results do not mean that columns are all oriented in the same direction in the plane of the substrate (homogeneous alignment) but rather that their stacking along the substrate normal is regular in the entire sample. In the plane of the substrate, the columns are likely to be curved as has been previously observed by AFM for **2**.¹³

Alignment behavior of the blends can once again be divided into the three regions. POM observations (Figure 6) show that above $x = 0.925$, planar alignment is found, similar to compound **2**. From $x = 0.90$ to $x = 0.40$, the columns align homeotropically on the substrate. This alignment is once again characterized by an absence of texture. From $x = 0.30$ to $x = 0.05$, planar alignment is observed. Similarly to what was seen for confined samples, the domain size decreases gradually throughout this concentration range.

X-ray diffraction measurements also confirmed these observations. For compositions $x = 0.975$ and $x = 0.95$, a similar trend to that of **2**, i.e., enhanced intensity of 20 reflection compared to 11 reflection, is observed (Figure 8). Preferential orientation is so apparent for $x = 0.975$ that not only intensity of 20 and 40 reflections increases significantly but even the 60 reflection can be observed (not shown in Figure 8). Similarly to **2**, these compositions exhibit a planar alignment where the shorter side of the rectangular unit cell is parallel to the substrate plane.

For compositions from $x = 0.925$ to $x = 0.40$, which exhibit a Col_h phase at room temperature (except $x = 0.925$ which is at the limit of the Col_r – Col_h transition), a dramatic decrease of the 10 reflection is observed (Figure 9) together with the emergence of a (rather diffuse) reflection corresponding to the π -stacking distance (see Figure S6 in the Supporting Information). The spread and low intensity of the latter indicate a low

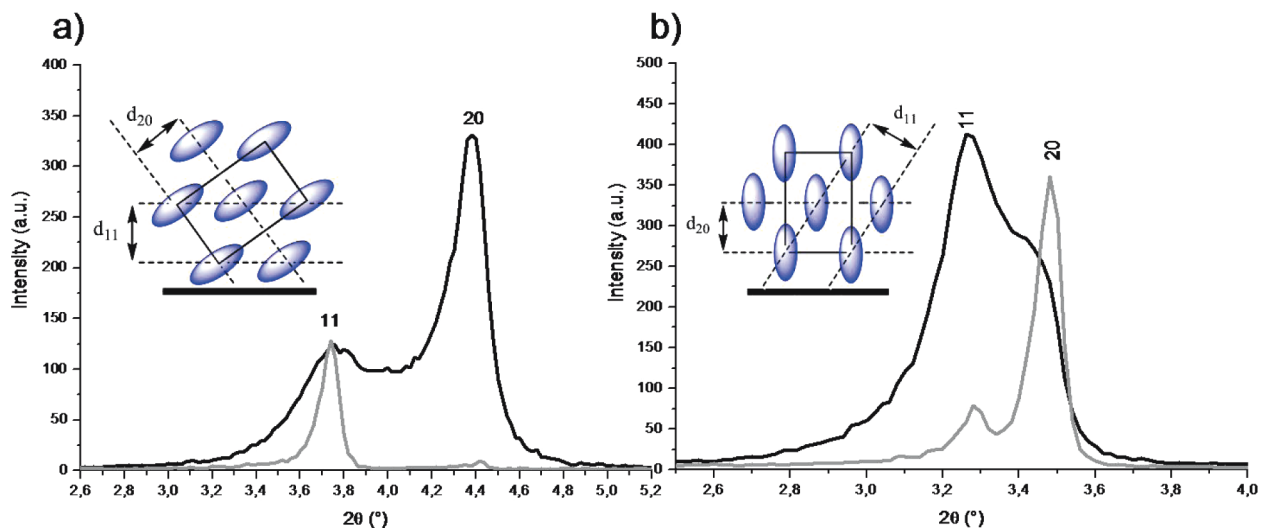


Figure 7. Comparison of the low-angle region of X-ray diffraction patterns measured at room temperature before (black) and after (gray) isotropization for (a) **1** and (b) **2**. Insets represent schematic orientation of the rectangular unit cell toward the substrate in both cases.

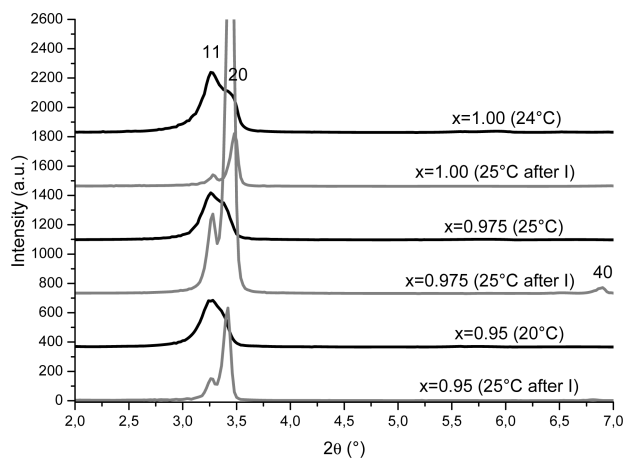


Figure 8. Low-angle region of X-ray diffraction patterns measured at room temperature before (dark lines) and after (gray lines) isotropization (I) for compositions $x = 0.95$, $x = 0.975$, and **2** ($x = 1.00$).

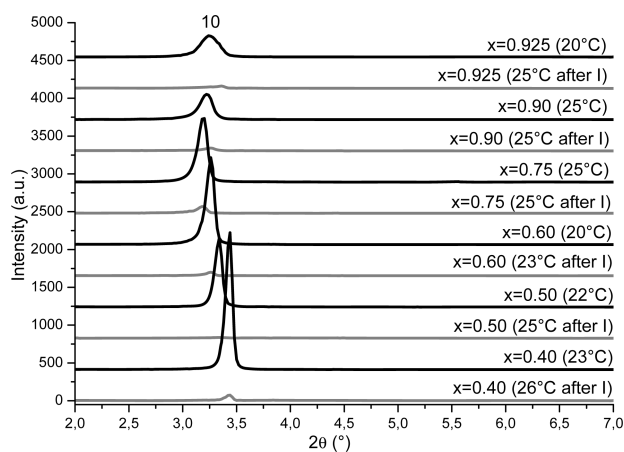


Figure 9. Low-angle region ($2-7^\circ 2\theta$ range) of X-ray diffraction patterns measured at room temperature before (black lines) and after (gray lines) isotropization (I) for compositions from $x = 0.925$ to $x = 0.40$.

stacking order within the columns, as in the case of the two pure constituents. This behavior is consistent with homeotropic alignment (columnar axis perpendicular to the substrate surface), since in this case only the $00L$ reflections should be observed. The remaining intensity of the 10 reflection which is observed for all compositions can be attributed to low level of misalignment.

Finally, from $x = 0.30$ to $x = 0.05$, no significant changes of the relative intensities of the 11 and 20 reflections or increase of the π -stacking reflection intensity could be observed between X-ray diffraction patterns measured before and after isotropization. This indicates a planar alignment with no particular orientational preference of the unit cell toward the substrate plane. This result is in agreement with the small birefringent domains observed by POM for these compositions.

Discussion

From the results collected here, it appears that columnar hexagonal arrangement induces homeotropic

alignment while columnar rectangular mesophase favors planar alignment. This is notable when looking at phase and alignment alternations as a function of blend composition. Indeed, homeotropic alignment has systematically been observed in blends presenting Col_h phase and planar alignment in blends presenting Col_r phase for samples annealed on one substrate as well as those sandwiched between two substrates. A similar correlation can also be made from observation of mesophase and alignment changes as a function of temperature for compositions from $x = 0.975$ to $x = 0.925$. Homeotropic alignment was in fact evidenced, both by POM (one substrate) and XRD, at temperatures above the Col_r – Col_h transition (see Figure S7 in the Supporting Information). This alignment is then broken on cooling past the Col_h – Col_r transition, thus yielding planar alignment of the columns. Pseudohomeotropic alignment observed for **2** and compositions rich in **2** in the Col_r mesophase, for samples sandwiched between two substrates, constitutes a special case in which the homeotropic alignment adopted at high temperature in the Col_h phase is preserved (“frozen in”) upon cooling to room temperature. The slightly birefringent characteristic textures presented by such an alignment stem from the fact that columns in the Col_r phase present a slight tilt with respect to the normal to the substrate surface.^{13,38} This pseudohomeotropic alignment would therefore constitute a kinetically favored arrangement of the mesophase and for those compositions, removal of the upper substrate along with reannealing leads to planar alignment at room temperature.^{13,38}

The present work thus evidence what has been previously observed experimentally for different discotic mesogens,^{7,12,13,15,21–28} i.e., Col_h arrangement is a necessary prerequisite for homeotropic alignment. It was demonstrated in a previous study by Grelet and Bock¹² that the alignment of columns in discotic mesogens exhibiting Col_h mesophase on an open surface resulted from an antagonist preferential orientation of the molecules. A face-on orientation of disks was found to be more favorable at the substrate-LC interface, whereas an edge-on orientation would prevail at the LC-air interface.^{12,40} It is then assumed that, as the growth of the LC material preferentially starts on the substrate, for a given cooling rate, homeotropic alignment could be kinetically favored for thick films, whereas stable planar alignment would be observed for thin films. Our results are in complete agreement with this explanation in the case of samples exhibiting Col_h mesophase, as thick films are only considered here (a few micrometers thick) and homeotropic alignment is always obtained. On the other hand, planar alignment has been reported for compound **2** when thin films (hundreds of nanometers thick spin-coated films) are considered.¹³ This work also suggests that it is the nature of the mesophase that governs the type of alignment exhibited when specific interactions between the

(39) Lu, G.; Li, L.; Yang, X. *Adv. Mater.* **2007**, *19*, 3594–3598.

(40) Mouthuy, P.-O.; Melinte, S.; Geerts, Y. H.; Nysten, B.; Jonas, A. M. *Small* **2008**, *4*, 728–732.

substrate and the rigid cores (or the alkyl chains) can be ruled out. It has indeed been thoroughly demonstrated by De Cupere et al.¹³ that the alignment behavior was independent from the nature of the substrate, in the specific case of **2** and this conclusion could be extended to all blends studied here since polarized optical microscopy observations (glass substrate) and X-ray diffraction measurements (aluminum substrate) are in full agreement. It is also important to note that the arrangement of discotic mesogens within the columns is different in Col_h and in Col_r mesophases. In fact, mesogens in Col_h phase present a face-to-face interaction with no tilt with respect to the column axis, while a slight tilt is present in Col_r phase. It is therefore understandable that only Col_h phase has the potential to form columns truly perpendicular to the substrate²⁸ and this is the reason why pseudohomeotropic alignment is only observed in the case of Col_r mesophase. It is thus possible that the differences in alignment behavior found for Col_h and Col_r mesophases are a consequence of the different positioning of the mesogens within the columns. A potential explanation for that fact could be that edge-on orientation of disks would now be preferred at the substrate-LC interface in the case of Col_r phase, thus promoting the growth of planarly aligned columns. The next step consists in evaluating the substrate-LC interfacial tension, for Col_r mesophases, of edge-on and face-on orientations^{40,41} and also their evolution as a function of the crystallographic planes to validate that hypothesis.

It was additionally pointed out that compounds **1** and **2** (and compositions rich in **2**) presented two different preferential orientations of the rectangular unit cell when in planar alignment on an open surface. Reasons for this phenomenon are not totally clear, although kinetics seem to play a role in the preferential alignment of compound **2** and compositions close to it when cooling down from Col_h mesophase (homeotropic alignment) to Col_r mesophase (planar alignment). It has indeed been observed by X-ray diffraction (see Figure S8 in the Supporting Information), that the respective amount of the preferential 20 oriented domains depends on the annealing time in the isotropic phase.

Finally, this work implicitly shows the importance of the absence of impurities such as side or degradation products that would perturb the phase diagram to allow proper investigation of the molecular alignment of discotics. Indeed, we can see that only a minimal amount of **1** has to be mixed with **2** to break its molecular alignment. As an example, on a single substrate, homeotropic alignment is observed for $x = 0.925$, whereas planar alignment is exhibited by pure **2**.

Conclusions

The aim of the present work was to improve the understanding of alignment behavior of discotic liquid

crystalline materials, and especially to relate the type of mesophase observed to a particular type of alignment. In order to achieve these goals, a phase diagram of blends of two miscible phthalocyanine mesogens (compounds **1** and **2**), presenting different mesophases and thermotropic behavior, was constructed. It showed a continuous evolution of transition temperatures, as well as a continuous transformation from one type of mesophase to the other, thus confirming the solid-state miscibility of both compounds in all proportions. In particular, Col_r-Col_h transitions that have been observed as a function of the composition are characterized by a continuous reversible distortion of the Col_r/Col_h lattices, as is also the case for the Col_r-Col_h transition observed for **2** upon heating.

The evolution of alignment as a function of composition has been probed by POM and XRD measurements for samples deposited on one substrate and confined between two substrates. It appears that homeotropic alignment is systematically adopted for mixed samples which exhibit Col_h phases, whereas planar alignment is preferred for Col_r samples. The evaluation of the interfacial tension of the two molecular orientations at the substrate-LC compound interface should be undertaken to explain this observation in terms of thermodynamic parameters. An essential conclusion of this work is that a Col_h mesophase is a necessary condition for observing homeotropic alignment. This conclusion holds true in the absence of specific substrate-LC interactions.

Acknowledgment. This work has been financially supported by the European Union (FP6-STAG STRP 033355), the Belgian Federation Science Policy Office (PAI SF2), and the Belgian National Fund for Scientific Research (FNRS). O.D. is a FRIA research fellow.

Supporting Information Available: Complete refs 29 and 31. Transition temperature and enthalpy change for all blend compositions. Phase diagram of binary system **1** and **2** including temperature transitions on heating and on cooling. Low-angle region of the X-ray diffraction patterns of the Col_r phase of compositions from $x = 0.925$ to $x = 1.00$. X-ray diffraction patterns as a function of the temperature of compositions $x = 0.925$ and $x = 0.95$. Low-angle region of the X-ray diffraction patterns of the Col_h phase of compositions from $x = 0.40$ to $x = 1.00$. Evolution of unit cell surface as a function of composition. High-angle region of the X-ray diffraction patterns measured at room temperature before and after isotropization for compositions from $x = 0.40$ to $x = 0.925$. Low-angle region of the X-ray diffraction patterns measured before and after isotropization for compositions from $x = 0.925$ to $x = 0.975$ in the Col_h phase. Low-angle region of the X-ray diffraction patterns measured at room temperature before and after isotropization for **2** at two annealing times in the isotropic phase. Lattice parameters and peak indexation for all blend compositions (PDF). This material is available free of charge via the Internet at <http://pubs.acs.org>.

(41) Mouthuy, P.-O.; Melinte, S.; Geerts, Y. H.; Jonas, A. M. *Nano Lett.* **2007**, *7*, 2627-2632.